

Latent gel electrolyte precursors for quasi-solid dye sensitized solar cells The comparison of nano-particle cross-linkers with polymer cross-linkers

T. Kato, A. Okazaki, S. Hayase*

Graduate School of Life Science and Systems Engineering, Kyushu Institute of Technology, 2-4 Hibikino, Wakamatsu-ku, Kitakyushu 808-0196, Japan

Received 13 March 2005; received in revised form 6 June 2005; accepted 13 July 2005

Available online 19 August 2005

Abstract

New latent gel electrolyte precursors (Precursor 1) consisting of ionic liquids and latent gelators are reported. The gelators are composed of poly(vinylpyridine) (PVP) and di-carboxylic acids. Gelation is caused by the reaction between PVP and di-carboxylic acid. Precursor 1 is liquid and is injected into cells and porous TiO₂ electrodes. Because of the latent properties, the viscosity of Precursor 1 does not increase at room temperature. After the Precursor 1 is injected into cells and into porous TiO₂ layers, the cell is heated at 90 °C. Solidification occurs swiftly. The latent mechanism is discussed. The trend of photo-voltaic performance for the cell filled with Precursor 1 before and after gelation was compared with that for the cell filled with previously reported latent gel electrolyte Precursor 2 composed of nano-particles and di-carboxylic acids. Photo-voltaic performance for the former decreased after quasi-solidification, but the latter did not. This is explained by insufficient phase-separations of gelator backbone from ionic liquid electrolytes after solidification.

© 2005 Elsevier B.V. All rights reserved.

Keywords: Dye sensitized solar cells; Nano-particle; Electrolyte; Quasi-solid; Gel electrolytes; TiO₂; Nano; Chemically cross-linked gel; Polyvinylpyridine; Silica; photo-conversion; Diffusion coefficient; Phase-separation; Phase-segregation

1. Introduction

Dye sensitized solar cells (DSC) have attracted interests because of high photo-energy conversion efficiencies and low cost cell fabrication processes [1]. One of the problems remaining is solidification of liquid electrolytes. All solid type DSCs with organic and inorganic conductive materials and polymer electrolytes have been reported [2–12]. We have focused on gel electrolytes using ionic liquid type electrolytes [13–17]. Because of the less volatility of these ionic liquids, vapor pressures for the solidified electrolytes are minimized. There are a lot of reports on DSCs containing ionic liquid type gel electrolytes [18–29]. Recently, gel electrolytes containing nano-particles have been paid attention because these soft gels do not decrease the photo-voltaic performances after solidification [12,26–30]. Graetzel and co-workers have reported ionic liquid type electrodes

containing silica nano-particles [26–28]. Yanagida and co-workers have also reported composite ionic gel electrolytes containing TiO₂ nano-particles [29]. These gel electrolytes are called physically cross-linked gels. Gelations are brought about by hydrophobic and hydrophilic interactions of gelators. They are originally solid at room temperature. Therefore, they are injected into cells at high temperatures, where the gel electrolytes become liquid. They are also injected into porous TiO₂ layers by diluting the gel electrolytes with volatile organic solvents, followed by heated in order to remove these solvents. We have reported chemically cross-linked gel electrolytes based on ionic liquid types for the first time [13]. Gelations were brought about by the chemical reaction between poly(vinylpyridene) (PVP) and tetrakis(bromomethyl)benzene. Gel electrolyte precursors were low viscosity-liquids, which enable the precursors to be injected into cells and nano-pores in TiO₂ layers even at room temperatures. Gelation was carried out in the cell directly at 80 °C. In addition, they exhibited high efficiencies associated with phase-separation of the gelator backbones

* Corresponding author.

E-mail address: hayase@life.kyutech.ac.jp (S. Hayase).

from ionic liquid type electrolytes. This is one of the easiest solidification methods to fabricate quasi-solid dye sensitized solar cells. However, once the precursor is prepared, the viscosity of the precursor starts to increase even at room temperature. This makes it difficult to make large cells because the viscosity gradually increases during the insertion into the cells. In order to solve this problem, we have reported latent gel electrolyte precursors consisting of nano-particles and di-carboxylic acids as gelators [30]. Gelation occurs by the reaction between nano-particles and di-carboxylic acids. The photo-conversion efficiency for the quasi-solid dye sensitized solar cell reached 7% [30]. The precursor was low viscosity-liquid. The viscosity of the precursor did not increase during storage or impregnation into cells at room temperature. This made it possible to fill the large cell fully with the precursors. The electrolyte precursor was solidified at around 90 °C swiftly. The latent means that reaction activities are hidden at room temperature. But the reaction (solidification) occurs swiftly when temperature reaches a certain limit. In this manuscript, we report that the latent properties are also brought about by poly(vinylpyridine) instead of nano-particles. The difference in photo-voltaic performances between gel precursor containing polymers and gel precursor containing nano-particles is reported. In addition, essential items to keep high photo-conversion efficiency after solidification are discussed.

2. Experimental

Compositions for gel precursors are summarized in Table 1. Electrodes containing ionic liquids are abbreviated as ILE1 and ILE2. Poly(vinylpyridine), di-carboxylic acids, tetra(bromomethyl)benzene (B4Br) were purchased from Sigma–Aldrich Corporation. Silica nano-particle (300) was obtained from Japan Aerogel Corporation.

Methylpropylimidazolium iodide (MePrImI) was purchased from Shikoku Kasei Corporation. A gel precursor, ILE1-C16-PVP (Table 1), was prepared as follows. PVP was dissolved in ILE1 at 90 °C and the mixture was cooled to room temperature. C16 was separately added in ILE1. The mixture was heated at 90 °C and cooled to room temperature. The two solutions were mixed at room temperature mechanically. Gelation of the precursors was observed visually after the mixture was heated to 90 °C.

Viscosity change during storage at 25 °C was measured by Brook Field-Model viscometer. Phase-transition of gel electrolytes were monitored with differential scanning calorimeter (Simadzu-model DSC-60).

Ti-nanoxide D paste (Solaronix SA) was coated on SnO₂/F layered glasses (30 Ω/sq, Nippon Sheet Glass Co. Ltd). The substrates were baked at 450 °C to fabricate 9 μm thickness of TiO₂ layers. The substrates were immersed in *cis*-Di(thiocyanato)-*N,N'*-bis(2,2'-bipyridyl-4,4'-di-carboxylato)ruthenium(II) (Kojima Kagaku) solution in ethanol (0.1%). Pt sputtered SnO₂/F layered glass substrates were employed as counter electrodes. A plastic sheet (HIMILAN, Mitsui-Dupont Co. Ltd, 50 μm) was inserted between the TiO₂ electrode and the counter electrode as spacers. A gel precursor was injected in the cell at room temperature. Then the cell was heated at 90 °C for 1 min. The cell area was 0.25 cm². Photo-electrochemical measurements were performed using a solar simulator (YSS-50A, Yamashita Denso Co. Ltd., AM 1.5, 100 mW/cm²). The light intensity was monitored with a polysilicon illuminometer.

The diffusion coefficient for I₃⁻ species was measured by the method described in the previous literature [31,32]. The symmetrical cells, sandwiched with two sputtered or thermally deposited Pt electrodes fabricated on SnO₂/F layered glass substrates, were used for the measurement. The cell gap was controlled to be 50 μm. Electrolytes were inserted in the cell and the cell was sealed. The electrode size was

Table 1
Abbreviations and composition of gel electrolyte precursors

| Abbreviation | Ionic liquid type electrolyte | | | | | Latent gelator | | | |
|--------------|-------------------------------|------------------------|---------------------|----------|----------------------------------|------------------------|--------------------------|--------------------------|----------|
| | MePrImI (wt%) ^a | H ₂ O (wt%) | I ₂ (mM) | Lil (mM) | <i>t</i> -BuPy (mM) ^b | PVP (wt%) ^c | Si300 ^d (wt%) | Di-carboxylic acid (wt%) | Gelation |
| ILE1 | 100 | 5 | 300 | | | | | | – |
| ILE1-C6-PVP | 100 | 5 | 300 | | | 2 | | C6 ^e 4 | NG |
| ILE1-C9-PVP | 100 | 5 | 300 | | | 2 | | C9 ^f 4 | NG |
| ILE1-C12-PVP | 100 | 5 | 300 | | | 2 | | C12 ^g 4 | Gelled |
| ILE1-C16-PVP | 100 | 5 | 300 | | | 2 | | C16 ^h 4 | Gelled |
| ILE2 | 100 | 5 | 300 | 500 | 580 | | | | – |
| ILE2-C16-300 | 100 | 5 | 300 | 500 | 580 | | 3 | C16 ^h 3 | Gelled |

^a Methylpropylimidazolium iodide.

^b *t*-Butylpyridine.

^c Poly(vinylpyridine).

^d Silica nano-particle, (Nippon Aerogel) 7 nm diameter.

^e HOCO(CH₂)₄COOH.

^f HOCO(CH₂)₇COOH.

^g HOCO(CH₂)₁₀COOH.

^h HOCO(CH₂)₁₄COOH.

1 cm². The voltage was swept from 0 to +1 V. When the voltage increased from 0 to 1 V, the current went up and reached a constant value corresponding to the limiting current. The diffusion coefficient was calculated by using the following formula [31,32].

$$D = \frac{I_{\text{lim}}d}{(2nFC)}$$

D , diffusion constant; I_{lim} , limiting currents; d , cell gap; n , the number of electrons (2); F , Faraday constant; C , initial I_2 concentration.

Electron diffusion coefficient in TiO₂ layers were estimated with intensity modulated photo-current spectroscopy (IMPS) [33–35]. These samples were exposed to 680 nm light by use of a laser diode (Lab Lasers, Coherent Japan Inc.). The laser diode was the source of both bias and modulated light. A NF Corporation frequency response analyzer Model 5020 was used to control light modulation and to measure the modulation of photo-potential. The current was measured by a Hokuto Denko Model HA-151 potentiometer. The amplitude of the sinusoidal modulation of the light intensity had an average value of 0.05 I_0 . Electron diffusion coefficient (D_e) was estimated by the frequency of minimum imaginary component in IMPS complex plane plot (f_{min}) as follows:

$$D_e = d^2 2\pi f_{\text{min}}$$

where d stands for TiO₂ thickness [35].

3. Results and discussion

3.1. Latent property

Table 1 summarizes electrolyte compositions. ILE1 stands for ionic liquid type electrolytes without gelators. Latent gelators, PVP and di-carboxylic acid, were added into ILE1 as shown in Table 1. When ILE1-C12-PVP and ILE1-C16-PVP were stored at room temperature, an increase in the viscosity was not observed as shown in Fig. 1. However, they solidified within 30 s when they were heated at 90 °C. ILE2-C16-300

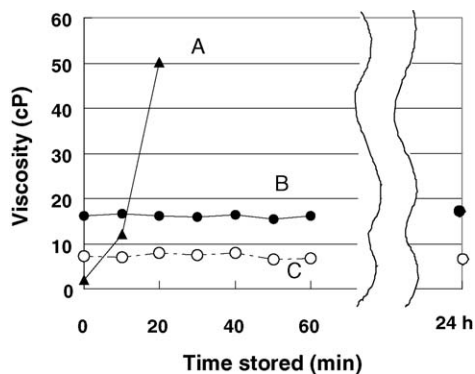
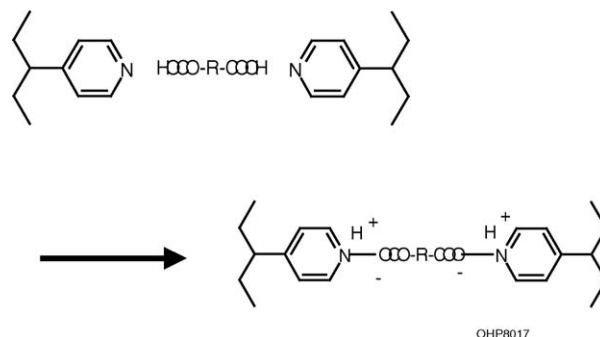


Fig. 1. Relationship between viscosity and time stored at room temperature. A, ILE 1-B4Br-PVP; B, ILE 1-C16-PVP; C, ILE 1-C12-PVP.



Scheme 1. Reaction of PVP with carboxylic acids for gelation.

showed the same behaviors. The initial viscosity was 12 cP and the viscosity did not change after the precursor was stored for 60 min at room temperature. Gelation was caused by the cross-linking reaction of PVP with di-carboxylic acids as shown in Scheme 1. The mechanism on the latent gelators is shown in Fig. 2. PVP is homogeneously dissolved in ILE1. However, C16 is phase-separated from ILE1 and dispersed uniformly at room temperature Fig. 2(1). PVP does not react with the phase-separated C16 at room temperature. When this is heated at 90 °C, phase-transition of C16 occurs and C16 becomes dissolved into ILE1. Immediately after the dissolution, C16 reacts with PVP to cause solidification Fig. 2(2).

In this connection, we have already reported the chemically cross-linked gels consisting of tetrakis(bromomethyl)benzene (B4Br) and PVP (ILE1-B4Br-PVP) [13]. This did not exhibit latent properties. The gelation was brought about by the reaction of B4Br with PVP. In this case, when the two gelators, B4Br and PVP, were mixed in ILE1 at room temperature, the viscosity started to increase gradually and reached 50 cP within 20 min as shown in Fig. 1. In the case of ILE1-C6-PVP and ILE1-C9-PVP, immediately after PVP solution in ILE1 was mixed with C6 or C9 solution in ILE1, precipitation occurred inhomogeneously. C6 and C9 were homogeneously dissolved in ILE1 and made clear solutions. Because of this, cross-linking reactions between PVP and C6 or C9 occurred instantaneously after they were mixed. This would cause inhomogeneous precipitation. We have already reported new latent gel electrolyte precursors consisting of

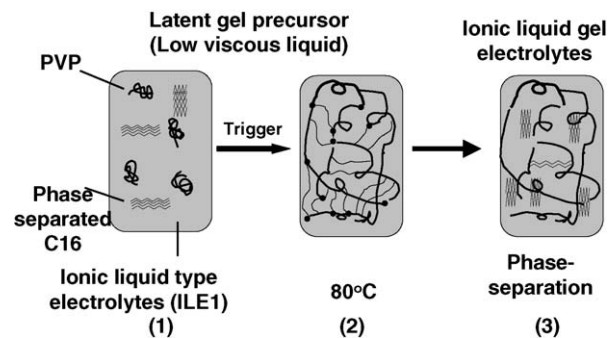


Fig. 2. Mechanism for solidification of ILE 1-C16-PVP. (1) Room temperature; (2) 90 °C and (3) room temperature.

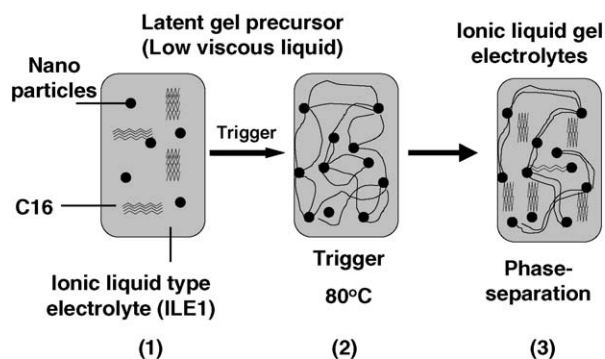


Fig. 3. Mechanism for solidification of ILE 2-C16-300. (1) Room temperature; (2) 90 °C and (3) room temperature.

nano-particles and di-carboxylic acids as gelators [30]. The reaction scheme is the same as that for ILE1-C16-PVP as shown in Fig. 3. The difference between Figs. 2 and 3 is in the point whether or not one of cross-linking reagents is soluble in ionic liquids at room temperature. A cross-linker, PVP, was soluble in ionic liquid type electrodes uniformly in Fig. 2. However, a cross-linker, nano-particle, was insoluble and dispersed uniformly in Fig. 3. From this experiment, it was found that uniformly dissolved PVP also worked for latent gelators.

3.2. Photo-voltaic performance and diffusion coefficient of I_3^- in electrolytes and electron diffusion coefficient in TiO_2 layers

Table 2 shows the photo-voltaic performances for these DSCs. ILE1 does not contain LiI and *t*-butyl pyridine which are contained in ILE2, because they inhibit gelation. Therefore, in this manuscript, the trend of photo-voltaic performance before and after gelation is discussed each other. The efficiency of ILE1 was 5.2%. After gelation, the efficiency decreased to 4.4% for Gelled ILE1-C16-PVP and 3.4% for Gelled ILE1-C12-PVP. These decreases in

Table 2
Photo-voltaic performances

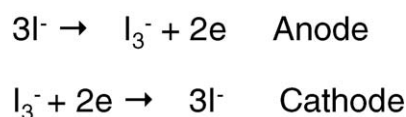
| | Gelled ILE1-C12-PVP | Gelled ILE1-C16-PVP | Gelled | | |
|---------------------------|---------------------|---------------------|--------|--------------|------|
| | | | ILE1 | ILE2-C16-300 | ILE2 |
| Efficiency (%) | 3.4 | 4.4 | 5.2 | 5.4 | 5.2 |
| FF | 0.52 | 0.55 | 0.65 | 0.60 | 0.63 |
| Voc (V) | 0.58 | 0.60 | 0.55 | 0.63 | 0.67 |
| Jsc (mA/cm ²) | 11.28 | 13.43 | 14.39 | 14.4 | 12 |

Table 3
 I_3^- diffusion constants in electrolytes and electron diffusion coefficient in TiO_2 layers contacting electrolytes

| | Gelled ILE2-C16-300 | ILE2 | Gelled ILE1-C12-PVP | Gelled ILE1-C16-PVP | ILE1 |
|--|---------------------|------|---------------------|---------------------|------|
| D_e^a (cm ² /s) $\times 10^{-5}$ | 3.63 | 2.93 | – | 2.24 | 3.58 |
| $D(I_3^-)^b$ (cm ² /s) $\times 10^{-6}$ | 1.01 | 1.04 | 0.83 | 0.89 | 1.2 |

^a Electron diffusion coefficient.

^b I_3^- diffusion coefficient.



Scheme 2. Reaction mechanism in electrolytes.

efficiencies were associated with decreases in fill factor (ff) and short circuit current (Jsc). After gelation, FF values decreased in the following order: ILE1 (FF 0.65), Gelled ILE1-C16-PVP (0.55), Gelled ILE1-C12-PVP (0.52). Jsc values also decreased in the following order: ILE1 (Jsc 14.39 mA/cm²), Gelled ILE1-C16-PVP (13.43 mA/cm²), Gelled ILE1-C12-PVP (11.28 mA/cm²). In the case of Gelled ILE2-C16-300, the efficiency increased from 5.2% (ILE2) to 5.4% after gelation. These results contrast the role of silica nano-particle with that of soluble PVP.

Ion-diffusion should be mostly affected after solidification of electrolytes. On the anode, I^- gives electron to form I_3^- (Scheme 2). On the cathode, I_3^- obtains electron to form I^- . I_3^- and I^- diffuse in electrolytes to carry electrons. Large size I_3^- species are considered to determine limiting currents in the electrolytes [31,32]. Therefore, I_3^- diffusion coefficient values in solidified electrolytes were evaluated. They are summarized in Table 3.

I_3^- diffusion coefficient values for Gelled ILE1-C16-PVP and Gelled ILE1-C12-PVP were 0.89×10^{-6} and 0.83×10^{-6} cm²/s, which was lower than that for ILE1 (1.20×10^{-6} cm²/s). In the case of Gelled ILE2-C16-300 and ILE2, their I_3^- diffusion coefficient values were almost the same (1.01 and 1.04×10^{-6} cm²/s, respectively). Namely the I_3^- diffusion coefficient for the former case decreased, but that for the latter case did not vary. These changes in I_3^- diffusion coefficient corresponded to Jsc changes of solar cells after gelation.

These results lead the following conclusions:

- (1) The photo-voltaic performance for Gelled ILE2-C16-300 using nano-particles as gelator did not decrease after

solidification, but that for Gelled ILE1-C16-PVP using PVP as gelator did.

- (2) Photo-voltaic performance for Gelled ILE1-C12-PVP was worse than that for Gelled ILE1-C16-PVP.
- (3) Photo-voltaic performances after gelation was associated with I_3^- diffusion coefficients.

4. Discussion

4.1. Difference between ILE1-C16-PVP and ILE2-C16-300

We believe that decreases in the I_3^- diffusion constant after solidification is associated with the degree of phase-separation of gelator backbone from ionic liquids. In the case of ILE2 and Gelled ILE2-C16-300, gelators should be phase-separated much more remarkably than in the case of Gelled ILE1-C16-PVP, because 300 is silica nano-particle and is insoluble in ionic liquids. The phase-separation of gelator backbones from ionic liquid decreases interaction between gelator backbone and I_3^- . Because of this, I_3^- diffusion was not disturbed even after solidification.

DSC curves for Gelled ILE1-C12-PVP and Gelled ILE2-C16-30 are shown in Fig. 4. They have endothermic and exothermic peaks even after gelation. Endothermic peaks on heating correspond to phase-transitions of ordered structures to disordered structures such as melting points of crystals. Exothermic peaks on cooling are observed when disordered structures were changed to ordered structures such as crystallization. In the case of Gelled ILE2-C16-300, an endothermic peak on heating (91 °C) corresponds to the change from ordered structures to disordered structures. An exothermic peak on cooling (83 °C) corresponds to the changes from

Table 4
Phase-transitions of gel electrolytes

| | Endothermic (°C) | Exothermic (°C) |
|---------------------|------------------|-----------------|
| Gelled ILE2-C16-300 | 91 | 83 |
| Gelled ILE1-C16-PVP | 86 | 67 |
| C16 ^a | 99 | 92 |

^a Measured in MePrImI.

disordered structures to ordered structures (Table 4). This implies that long alkyl groups of C16 aggregated to make self-organized structures at 83 °C when this was cooled from 120 °C. On heating this aggregate structures became disordered structures at 91 °C. It is likely that these gelator-backbones are phase-separated uniformly from ionic liquid electrolytes on cooling. The phase-transition of Gelled ILE2-C16-300 was observed with reproducibility at 83 °C. However, the peak for Gelled ILE1-C16-PVP was observed at 67 °C with less reproducibility (Fig. 4 and Table 4). C16 had a exothermic peak at 99 °C. The endothermic peaks shifted from 99 to 91 °C for gelled ILE2-C16-300 and to 86 °C for Gelled ILE1-C16-PVP. The large temperature shifts of endothermic peaks for Gelled ILE1-C16-PVP on cooling suggest that taking the ordered structure was somehow disturbed after gelation. They suggest that Gelled ILE2-C16-300 developed structurally ordered-networks (Fig. 3(3)) more than Gelled ILE1-C16-PVP (Fig. 2(3)). It is likely that structurally ordered long alkyl chains are phase-separated from hydrophilic environment. This would explain why I_3^- diffusion coefficient for ILE1-C16-PVP decreased after solidification and that for ILE2-C16-300 did not decrease even after solidification. Insoluble nano-particle may support the phase-separation of alkyl chains.

Electron diffusion coefficient values for ILE2 and Gelled ILE2-C16-300 were 2.93×10^{-5} and 3.65×10^{-5} cm²/s

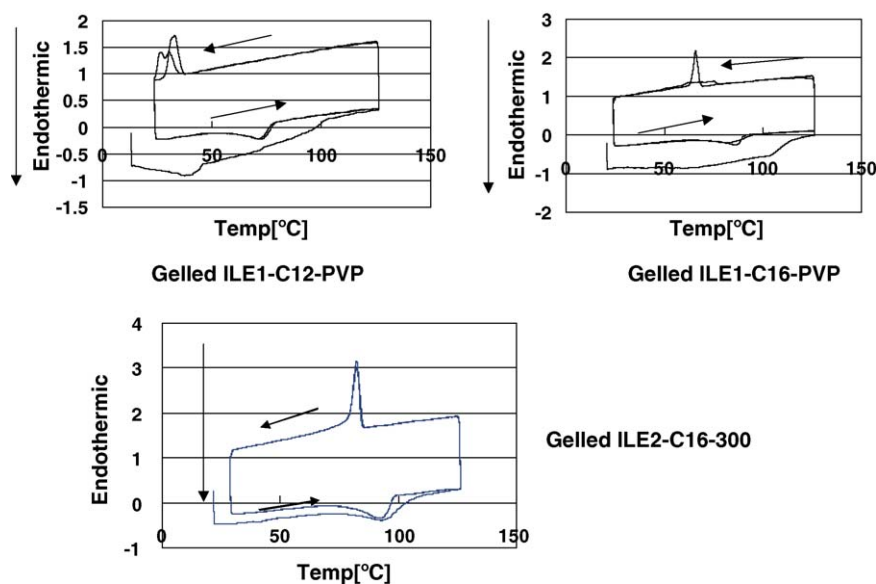


Fig. 4. DSC curves for gel electrolytes.

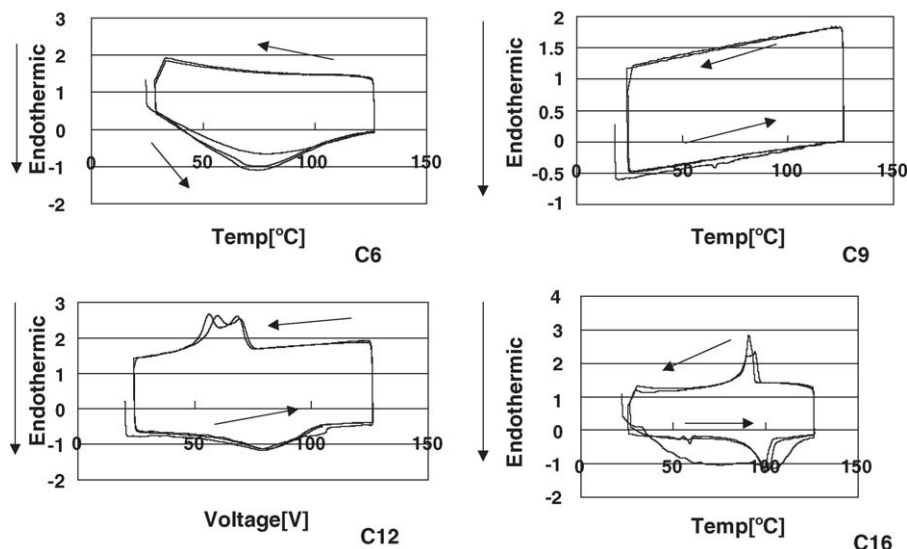


Fig. 5. DSC curves for di-carboxylic acids in methylpropylimidazolium iodide.

(Table 3). The fact that electron diffusion coefficient for gelled electrolytes increased was explained by the addition of di-carboxylic acids [30]. Nakade et al. have reported that electron diffusion coefficient increased in TiO₂ layers when TiO₂ particles were covered with dye molecules bearing carboxylic acids [36]. We have also reported that TiO₂ was modified with carboxylic acids, electron diffusion coefficient increased [17]. A part of di-carboxylic acids may modify the surface of TiO₂ layers. Electron diffusion coefficient values for ILE1 and Gelled ILE1-C16-PVP were 3.58×10^{-5} and 2.24×10^{-5} cm²/s. The decrease in electron diffusion coefficient in TiO₂ layers for solidified DSC can be explained by the addition of PVP as gelators. We have observed that electron diffusion coefficient decreased when TiO₂ was modified with *t*-butylpyridine [37]. This is one of the reasons for Jsc decrease after gelation, in addition to the decrease in I₃⁻ diffusion coefficient.

4.2. Difference between ILE1-C12-PVP and ILE1-C16-PVP

Gelled ILE1-C12-PVP also has endothermic and exothermic peaks. The exothermic peak on cooling appeared with less reproducibility as shown in Fig. 4. C12 had an endothermic peak at 79 °C and an exothermic peak at around 56–68 °C (Fig. 5 and Table 5). In the case of Gelled ILE1-C12-PVP, these peaks were at 72 and 26–32 °C. The exothermic peak

shifted to low temperature side by 30–36 °C after gelation. In the case of Gelled ILE1-C16-PVP and C16, the temperature shift in the exothermic peak was 25 °C after gelation. These results suggest that ordering of alkyl chains was somehow disturbed in Gelled ILE1-C12-PVP more than in Gelled ILE1-C16-PVP. The degree of phase-separation should be less in the case of Gelled ILE1-C12-PVP than in the case of Gelled ILE1-C16-PVP because of the shorter alkyl chains. This explains the lower I₃⁻ diffusion constant and lower Jsc for Gelled ILE1-C12-PVP than for Gelled ILE1-C16-PVP.

4.3. Latent properties depending on the chain length of di-carboxylic acids

Fig. 4 shows DSC curves of di-carboxylic acids in ionic liquid, methylpropylimidazolium iodide. DSC curves for C6 and C9 did not show endothermic and exothermic peaks corresponding to phase-transition. This means that C6 and C9 are completely dissolved in MePrImI and have disordered structures. This is why precipitation occurred immediately after C6 or C9 was added into PVP solution in ILE1. In the case of C12 and C16, exothermic and endothermic peaks corresponding to phase-transition were observed. It is likely that C12 and C16 are dispersed at room temperature in the form of ordered structures similar to the crystal structure. Because of the dispersed states at room temperature, precursors, ILE1-C12-PVP, ILE1-C16-PVP and ILE2-C16-300, kept low viscosity even after the C12 and C16 were mixed with PVP or silica nano-particle in ionic liquid electrolytes at room temperature. When they were heated, phase-transition of C12 and C16 occurred and they were dissolved into ionic liquid electrolytes. Immediately after they were dissolved into ionic liquids, solidification occurred.

Table 5
Phase-transitions of gel electrolytes

| | Endothermic (°C) | Exothermic (°C) |
|---------------------|------------------|-----------------|
| Gelled ILE1-C12-PVP | 72 | 26–32 |
| C12 ^a | 79 | 56–68 |

^a Measured in MePrImI.

5. Conclusion

In order for gel electrolyte precursors to exhibit latent properties, it is indispensable that gelator-monomers are phase-separated from ionic liquid solutions (or dispersed) at room temperature and the monomers change to form disordered structures at the temperature less than 90 °C, at less than which dye molecules are not damaged thermally. In order to keep high photo-energy conversion efficiencies after solidification, phase-separation of gelator backbones was very important. Phase-separation of gelators was caused more effectively by using nano-particles than by using PVP polymers. Insoluble nano-particle may support the phase-separation of alkyl chains. These latent gel electrolyte precursors are essential for fabrication of solidified large solar cells with high photo-conversion efficiencies.

Acknowledgements

This work is partially supported by Grant-in-Aid for Scientific Research on Priority Areas (417) from the Ministry of Education, Culture, Sports, Science and Technology (MEXT) of the Japanese Government.

References

- [1] A. Hagfeldt, M. Gratzel, *Chem. Rev.* 95 (1995) 49.
- [2] K. Tennakone, J. Bandara, P.K.M. Bandaranayake, G.R.A. Kumara, A. Konno, *Jpn. J. Appl. Phys. Part 2 Lett.* 40 (2001) L732.
- [3] G.R.A. Kumara, A. Konno, K. Tennakone, *Chem. Lett.* (2001) 180.
- [4] T. Taguchi, X.-T. Zhang, I. Sutanto, K. Tokuhira, T.N. Rao, H. Watanabe, T. Nakamori, M. Uragami, A. Fujishima, *Chem. Commun.* (2003) 2480.
- [5] K. Tennakone, G.R.A. Kumara, I.R.M. Kottegoda, V.P.S. Perera, P.S.R.S. Weerasundara, *J. Photochem. Photobiol. A: Chem.* 117 (1998) 137.
- [6] B. O'Regan, D.T. Schwartz, *J. Appl. Phys.* 80 (1996) 4749.
- [7] D. Gebeyehu, C.J. Brabec, N.S. Saricifci, D. Vangeneugden, R. Kiebooms, D. Vanderzande, F. Keinberger, H. Schindler, *Synth. Met.* 125 (2002) 279.
- [8] B. O'Regan, D.T. Schwartz, *Chem. Mater.* 7 (1995) 1349.
- [9] U. Bath, D. Lupo, P. Comte, J.E. Moser, F. Weissortel, J. Salbeck, H. Spreitzer, M. Graetzel, *Nature* 395 (1998) 583.
- [10] K. Tennakone, G.K.R. Senadeera, D.B.R.A. De Silva, I.R.M. Kottegoda, *Appl. Phys. Lett.* 70 (2000) 2367.
- [11] Y.J. Kim, J.H. Kim, M.-S. Kang, M.J. Lee, J. Won, J.C. Lee, Y.S. Kang, *Adv. Mater.* 16 (2004) 1753.
- [12] J.H. Kim, M.-S. Kang, Y.J. Kim, J. Won, N.-G. Park, Y.S. Kang, *Chem. Commun.* (2004) 1662.
- [13] S. Murai, S. Mikoshiba, H. Sumino, T. Kato, S. Hayase, *Chem. Commun.* (2003) 1534.
- [14] S. Mikoshiba, S. Murai, H. Sumino, S. Hayase, *Chem. Lett.* (2002) 1156.
- [15] S. Mikoshiba, S. Murai, H. Sumino, S. Hayase, *Chem. Lett.* (2002) 918.
- [16] Y. Shibata, T. Kato, T. Kado, R. Shiratuchi, W. Takashima, K. Kaneto, S. Hayase, *Chem. Commun.* (2003) 2730.
- [17] S. Sakaguchi, H. Ueki, T. Kato, T. Kado, R. Shiratuchi, W. Takashima, K. Kaneto, S. Hayase, *J. Photochem. Photobiol. A: Chem.* 164 (2004) 117.
- [18] S. Yanagida, S. Kambe, W. Kubo, K. Murakoshi, T. Wada, T. Kitamura, *Zeitschrift fur Physikalische Chemie Bd212* (1999) S.38.
- [19] K. Tennakone, G.K.R. Senadeera, V.P.S. Perera, I.R.M. Kottegoda, L.A.A. De Silva, *Chem. Mater.* 11 (1999) 2474.
- [20] E. Stathatos, P. Lianos, U.L. Stangar, B. Orel, *Adv. Mater.* 14 (2002) 354.
- [21] Y. Ren, Z. Zhang, S. Fang, M. Yang, S. Cai, *Sol. Energy Mater. Sol. Cells* 71 (2002) 253.
- [22] O.A. Ieperuma, M.A.K.L. Disssanayake, S. Somasundaram, *Electrochim. Acta* 47 (2002) 2801.
- [23] P. Wang, S.M. Zakeeruddin, J. Moser, M.K. Nazeeruddin, T. Sekiguchi, M. Gratzel, *Nat. Mater.* 2 (2003) 402.
- [24] W. Kubo, K. Murakoshi, T. Kitamura, S. Yoshida, M. Haruki, K. Hanabusa, H. Shirai, Y. Wada, S. Yanagida, *J. Phys. Chem. B* 105 (2001) 12809.
- [25] W. Kubo, T. Kitamura, K. Hanabusa, Y. Wada, S. Yanagida, *Chem. Commun.* (2002) 374.
- [26] P. Wang, S.M. Zakeeruddin, I. Exnar, M. Graetzel, *Chem. Commun.* (2002) 2972.
- [27] P. Wang, S.M. Zakeeruddin, P. Comte, I. Exnar, M. Graetzel, *J. Am. Chem. Soc.* 125 (2003) 1166.
- [28] E. Stathatos, P. Lianos, S.M. Zakeeruddin, P. Liska, M. Graetzel, *Chem. Mater.* 15 (2003) 1825.
- [29] H. Usui, H. Matsui, N. Tanabe, S. Yanagida, *J. Photochem. Photobiol. A: Chem.* 164 (2004) 97.
- [30] T. Kato, A. Okazaki, S. Hayase, *Chem. Commun.* (2005) 363.
- [31] N. Papageorgiou, W. Maier, M. Gratzel, *J. Electrochem. Soc.* 144 (1997) 876.
- [32] N. Papageorgiou, Y. Athanassov, M. Armand, P. Bonhote, H. Pettersson, A. Azam, M. Gratzel, *J. Electrochem. Soc.* 143 (1996) 3099.
- [33] G. Schlichthorl, S.Y. Hung, J. Sprague, A.J. Frank, *J. Phys. Chem. B* 101 (1997) 8141.
- [34] L.M. Peter, K.G.U. Wijayatha, *Electrochim. Acta* 45 (2000) 4543.
- [35] T. Yoshida, T. Oekermann, K. Okabe, D. Schlettwein, K. Funabiki, H. Minoura, *Electrochim. Acta* 47 (2002) 470.
- [36] S. Nakade, Y. Saito, W. Kubo, T. Kanzaki, T. Kitamura, Y. Wada, S. Yanagida, *Electrochim. Commun.* 5 (2003) 804.
- [37] S. Hayase, unpublished data.